INSTITUTE OF PHYSICS PUBLISHING SUPERCONDUCTOR SCIENCE AND TECHNOLOGY

Supercond. Sci. Technol. **18** (2005) 1489–1495 doi:10.1088/0953-2048/18/11/014

Microstructure origin of hot spots in textured laser zone melting Bi-2212 monoliths

F Lera[1,2], L A Angurel[1], J A Rojo[1], M Mora[1], S Recuero[2], M P Arroyo[2] and N Andrés[2]

[1] Instituto de Ciencia de Materiales de Aragón (CSIC-Universidad de Zaragoza), c/ María de Luna 3, 50018 Zaragoza, Spain

[2] Instituto de Investigación en Ingeniería de Aragón (I3A), Facultad de Ciencias, Universidad de Zaragoza, c/ Pedro Cerbuna 12, 50009 Zaragoza, Spain

Received 3 August 2005, in final form 20 September 2005
Published 7 October 2005
Online at stacks.iop.org/SUST/18/1489

Abstract

Hot spots are one of the main limitations in the development of large-scale high-power applications with superconducting materials. The application of digital speckle interferometry to detect inhomogeneous heating on ceramic superconductors allows the determining of a hot spot location in these materials before any damage is caused to the material. The technique detects deformations that are induced in the material due to dilatation, attaining a resolution of 0.45 μm/fringe. In this paper this technique has been applied to analyse the heating generation in Bi-2212 superconducting monoliths at room temperature and in operation conditions. In the first case a homogeneous heating is obtained, leading to a parallel fringe pattern. In the second case, a situation with an inhomogeneous heating origin has been detected. Once the position of this hot spot is determined, microstructure studies have been performed to determine which defects are responsible for hot spot generation.

1. Introduction

The development of superconducting fault current limiters (SFCL) is one of the possible industrial-scale applications of bulk high-temperature superconductors and has been addressed by several research groups worldwide [1–3]. The fault current limitation ability relies on a fast quench to the normal state, with a sufficiently short recovery time, that should take place simultaneously in a long path of superconductor. The performance of a resistive SFCL is critically dependent on the sample length involved in the transition [4, 5]. This leads to one of the main practical difficulties for SFCL fabrication: the existence of inhomogeneities on the superconducting properties along a current path, that can be several metres long, leads to non-simultaneous quench, generating hot spots that compromise overall performance and could even irreversibly damage the superconductor [6].

One alternative for developing superconducting materials adequate to be used in resistive SFCL is the fabrication of thick films with a large area and to machine them in a meander geometry [7]. A laser zone melting (LZM) method has been used to obtain a textured material with a planar geometry and an adequate critical current density value [8, 9]. This technique has been used to fabricate long well-textured $Bi_2Sr_2CaCu_2O_{8+\delta}$ (Bi-2212) monoliths with rectangular cross-sections and thick films on silver and MgO substrates [10]. As in other materials with similar characteristics, the appearance of hot spots is their main limitation in large-scale electrical applications.

The detection of such inhomogeneities in ceramic high-temperature superconductors to trace their origin, to optimize fabrication processes or to perform post production quality control is a difficult challenge. In order to measure the critical current distribution, the use of multiple electrical contacts in $V(I)$ characteristic measurements is a time-consuming, ineffective method useful only in the laboratory and for short samples. A possible alternative is to measure the perpendicular magnetic field component above current-carrying samples by scanning Hall probe magnetometry [11]. The appearance of hot spots has been also detected with acoustic emission [12].

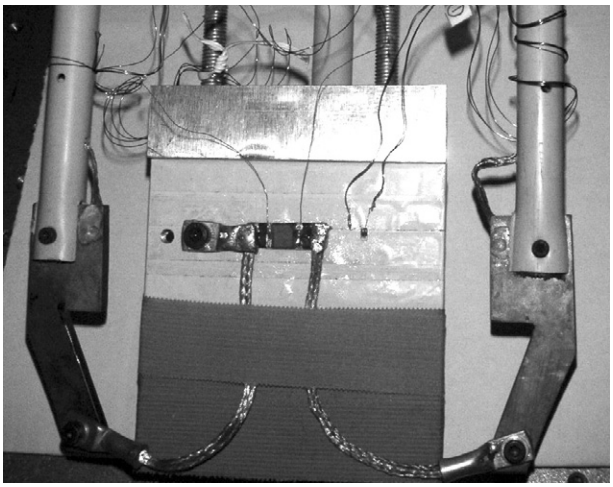

Figure 1. Photograph of the experimental sample arrangement with sample B anchored to the aluminium plate. Terminals for current and voltage measurements are also shown.

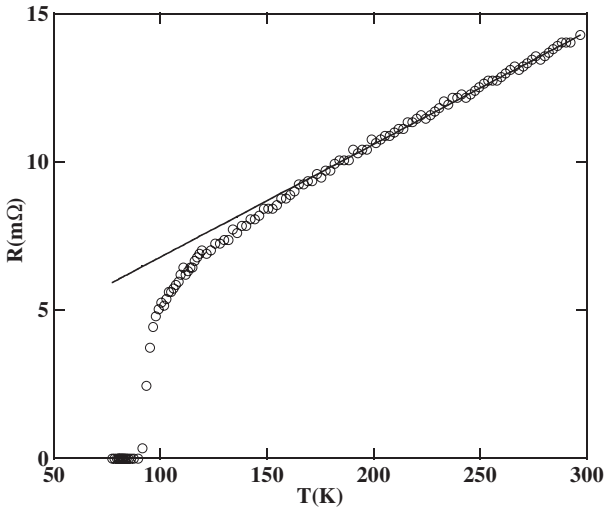

Figure 2. Measured DC resistance for sample A (symbols) and linear behaviour fit for $T > 160$ K.

This technique allows detecting the presence of a hot spot in high-temperature superconductor devices, but not its location. Detection by visual inspection of cryogen bubble generation [13] is not precise enough and not suitable for use in all cases. Recently, we have reported the application of digital speckle pattern interferometry (DSPI) [14] to detect inhomogeneous heating on superconducting ceramics. This is a contactless method that could be used to monitor large areas of the SFCL during service, locating hot spots well before irreversible damage takes place, for further research or for quality control.

In this paper we show the application of the technique to locate hot spots in Bi-2212 bulk melt-textured samples. Microscopic studies carried out on the samples revealed the existence and nature of the defects responsible for the hot spots detected with DSPI.

2. Low-temperature DSPI

DSPI is an interferometric technique that records on a CCD camera the interference of the light coming from the object and that coming from a reference wave. This interference is called a specklegram. Fringe patterns are obtained by comparing two different specklegrams recorded in two different states [15], an initial undeformed reference one and a later deformed state. The fringes correspond to phase differences, wrapped in the range 0–2π and mapped to a grey scale (black for 0 to white for 2π phase shift). The phase changes are directly related to the displacement in a direction determined by the recording geometry. From these fringes, after an unwrapping process, small deformation and/or displacements can be measured and digitally recorded in a fast, contactless, highly sensitive way over an area of several cm^2 [14].

There are difficulties to overcome in order to apply this technique to detect hot spots in superconducting samples in service conditions [14, 16]. Among these, the most demanding one is the need for a stable atmosphere around the sample under test, to minimize unwanted phase variations in the specklegram, due to liquid or gas movements. Thus, the

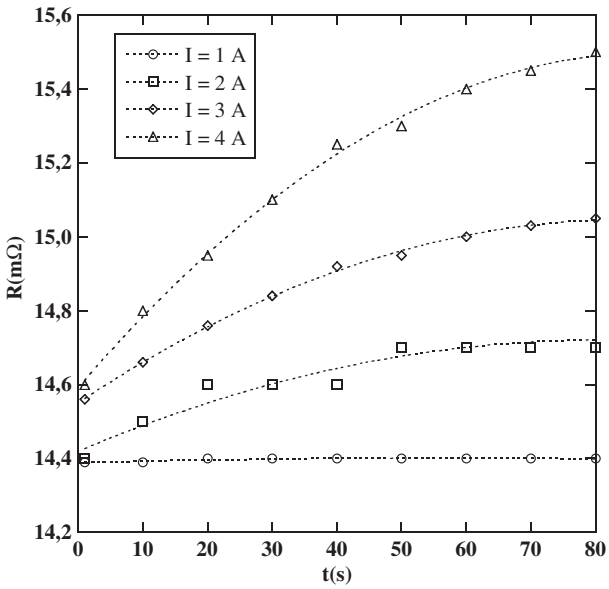

Figure 3. Time evolution of the DC resistance for sample A under different applied currents. The dotted lines are only guides for the eye.

sample instead of being cooled by immersion should be cooled by conduction, thermally anchored to a bulk aluminium piece that is itself partially immersed in an undercooled liquid nitrogen bath and in a low-pressure (10^{-1} atm) atmosphere (figure 1).

The arrangement is completed with thermometry, current leads and electrical contacts for simultaneous *in situ* voltage drop measurements. It is housed in a plated glass Dewar with clear windows for illumination and observation of the sample. In the experimental configuration used in this work, out-of-plane deformations of 0.45 μm/fringe are measured.

Before starting the experiments a calibration measurement is performed in order to be able to determine the sign of the displacement.

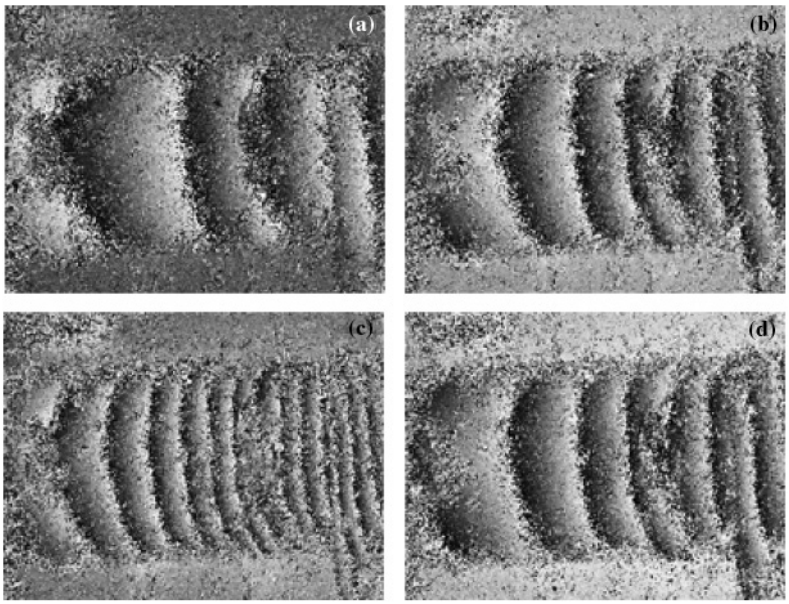

Figure 4. Time evolution of the fringe patterns in sample A with a current of 4 A: (a) Specklegram after 20 s with a resistance increment of 0.35 mΩ, (b) after 30 s and $\Delta R = 0.50$ mΩ and (c) after 80 s and $\Delta R = 0.9$ mΩ. In (d) the fringe pattern obtained with 3 A after 80 s ($\Delta R = 0.49$ mΩ) is presented. Compare it with (b).

3. Sample preparation and characterization

Detection of hot spots has been performed on textured Bi-2212 monoliths in the form of parallelepipeds with a nearly rectangular cross-section of 8 mm × 1–2.5 mm. The texturing process was produced using an LZM technique with a diode high-power laser emitting at 810 nm [8, 9]. The samples were processed in the horizontal plane using a transverse rate of 35 mm h^{-1} and a total laser power of 14 W. Silver plates have been used as support material, and they were heated at 400 °C with an electrical resistance furnace during the texturing process.

Results are presented in two samples. Because of the difference in density between the polycrystalline precursors and the textured zone-melted materials, in the case of sample A both surfaces were processed. This procedure was useful to avoid unsymmetrical deformation of the samples during thermal treatment, which would have resulted in excessive sample bending. The as-grown samples were isothermally annealed in air at 845 °C for 60 h to fully develop the superconducting Bi-2212 phase. In sample B, only a surface has been textured. The ceramic polycrystalline precursor that remained in the second surface was eliminated before annealing by carefully sanding the surface.

The form of the solidification profile determines how the grain orientation is modified inside the textured sample. These profiles show a pronounced vertical slope near the surface layers and a reduced, nearly horizontal, slope approaching the deeper thermally affected regions [9]. As the grains exhibit a strong tendency to grow in the direction perpendicular to the solidification interface, the pronounced slope in the solidification profile results in a better alignment of the grains in a thin layer of around 500 μm close to the sample surface. It has been observed that the critical current in these materials depends on the thickness of this well-textured region. For this reason, a laser machining of the surface [7] has been performed in sample B in order to eliminate the upper 300 μm of the sample between the two voltage contacts and to force the current to penetrate inside the sample, in the region with poorer texture.

Microstructural studies have been performed in polished samples using a JEOL 6400 SEM microscope equipped with an energy dispersive spectroscopy (Link-Analytical EDS) system.

Electrical transport measurements were performed using the conventional four-point probe configuration. Critical current (I_c) values were determined at 77 K using the 1 μV cm^{-1} criterion. Resistance as a function of temperature, $R(T)$, was measured using a DC current of 10 mA.

4. Room-temperature results

Initial experiments were performed at room temperature, when the sample can be considered as a homogeneous ohmic resistor. Thus, resistance changes induced by heating can be easily related to global temperature changes in the sample. Figure 2 shows the $R(T)$ dependence for sample A. The data for $T > 160$ K can be adjusted to a linear dependence $R(T) = 3{+}0.038T$ (mΩ). When a high current is applied to the sample, a transient heating process towards a steady-state temperature takes place. Figure 3 shows the evolution of the resistance values with time for different applied currents, between 1 and 4 A, for 80 s. Simultaneously, a series of specklegrams with 2 ms exposure times were recorded. Some of them, in the case of $I = 4$ A, are shown in figure 4. These show also a transient-like behaviour, with parallel fringes appearing, increasing in number towards a steady-state value.

A more detailed analysis shows that a high correlation exists between the number of fringes and the global temperature increase in the sample, showing that equal resistance changes lead to equal number of fringes, for equal

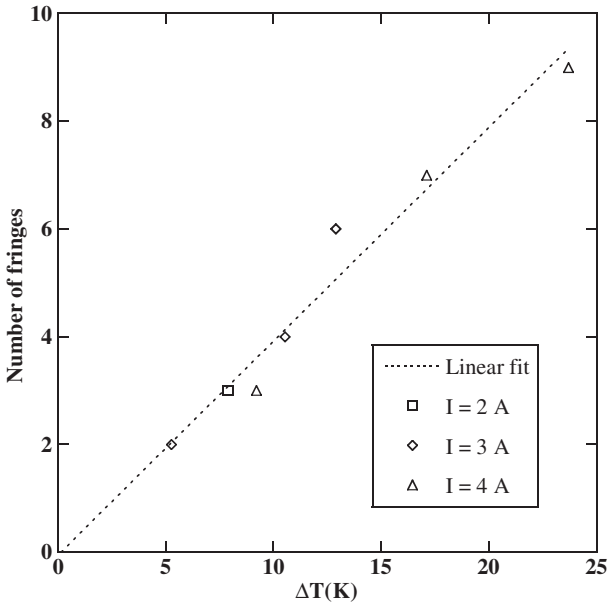

Figure 5. Number of fringes in the specklegram versus the global temperature increase. The slope of the linear fit is 180 nm K^{-1}.

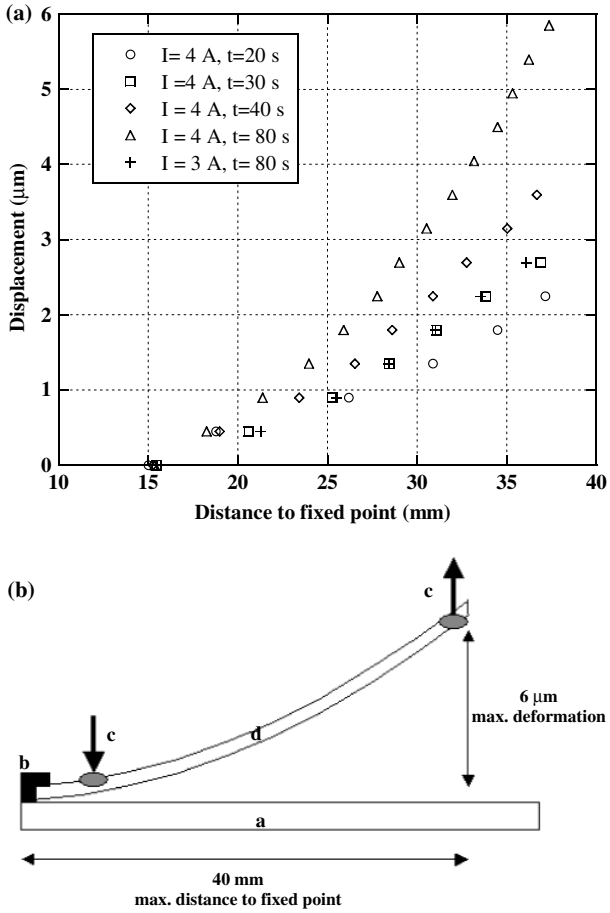

Figure 6. (a) Out-of-plane deformation as a function of the distance to the fixed point for different experimental conditions. (b) Schematic view of the deformation in the sample. a = cold plate, b = fixing screw, c = current leads, d = deformed superconducting plate.

or different applied currents. This is more evident comparing figures 4(b) and (d), in which the fringe patterns of two different experimental conditions that have produced a similar ΔR are presented. In particular, in figure 4(b) we observe the fringe pattern obtained with $I = 4$ A after 30 s ($\Delta R = 0.50$ mΩ) and in figure 4(d) the pattern observed with $I = 3$ A after 80 s ($\Delta R = 0.49$ mΩ). Both patterns look identical. From the above-mentioned high-temperature $R(T)$ linear relationship, the global sample temperature increase can be estimated from $R(t)$. The number of fringes present in each specklegram can be counted and is plotted versus this global temperature increase in figure 5, showing a deformation in the direction perpendicular to the sample of 180 nm K^{-1} for a point located at the rightmost position in the recorded images.

After phase unwrapping, the deformation for each point in the sample surface can be obtained. In figure 6(a) this is done for the specklegrams recorded at different times with an applied current of 4 A. Data for $I = 3$ A after 80 s are also included to observe the coincidence with those obtained for $I = 4$ A after 30 s. The sample leftmost end is tightly bonded to the aluminium plate by a screw, while the rightmost one is free to move (figure 6(b)). The results are consistent with the material bending due to the temperature difference between the rear and the front surfaces (figure 6(b)). In these experiments, the sample recovered its initial undeformed state several seconds after switching off the applied current, as can be observed by the disappearance of the fringes.

5. Low-temperature results

Low-temperature measurements have been performed on sample B. As has been mentioned, in this sample, in the central region between the two voltage contacts, a layer of 300 μm has been removed using a machining laser ablation process [7]. This layer corresponds to the region in which a better texture is obtained with the LZM process and, in consequence, this machining forces the current to penetrate inside the sample, where the grains have a poorer orientation and a higher amount of defects is expected to appear. This is reflected in the critical current value at 77 K that is reduced from 50 to 10 A. All the experiments have been performed after having allowed the sample to warm up to a temperature in which the critical current value has been reduced up to values lower than 2 A.

Figure 7 shows the evolution of the fringe pattern with time on applying a current of 15 A to the sample. In the beginning (figure 7(a)), the sample does not experience any deformation. After a given time ($t = 8.4$ s, figure 7(b)), the fringes start to appear. This time depends on the dissipation in the sample: with higher applied currents it is lower. They do not present a pattern of parallel fringes as was observed in room-temperature experiments; clearly we can observe that the new fringe pattern has its origin in one point. The time evolution of this pattern (figures 7(c) and (d)) correspond to new fringes that have their origin in this point. These fringes are associated with out-of-plane deformations caused by local heating originating at this point. The hot spot location is much more evident when sequentially acquired images are combined in a video stream. The details of the heat-induced deformation

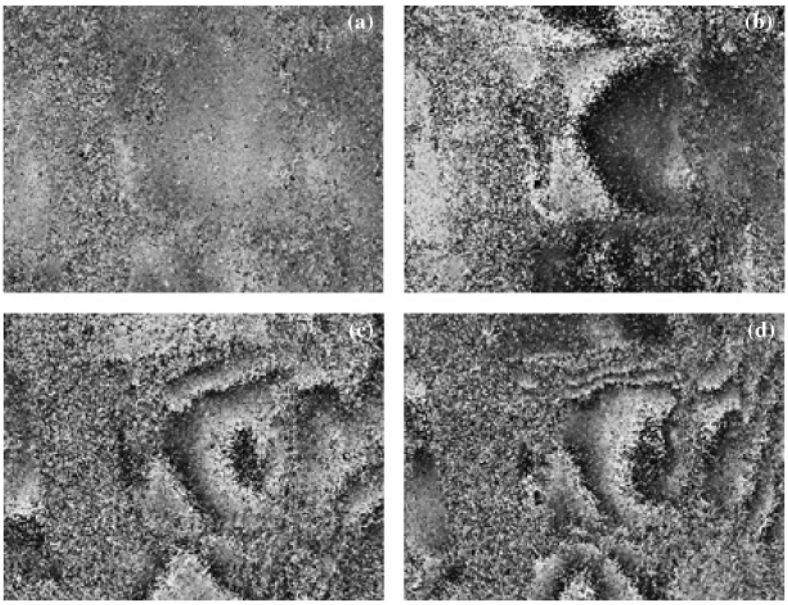

Figure 7. Evolution of the fringe pattern in sample B at a temperature in which $I_c < 2$ A. The applied current was 15 A and the patterns have been observed at (a) $t = 4.0$ s, (b) $t = 8.4$ s, (c) $t = 12.0$ s and (d) $t = 16.0$ s.

Figure 8. Fringe patterns recorded for a sample with $I_c = 2$ A under a 10 A current, at $t = 35$ s, showing two defects (marked with black crosses) separated 3 mm.

of a given sample depend on the mechanical characteristics of the sample and its fixing holder, and thus it is not possible in the present state of the technique to derive further details of the hot spot, apart from its position.

Figure 8 shows another example of fringe patterns recorded for a similar sample, with a critical current of 2 A, in this case after applying 10 A current for 35 s. Two different hot spots, separated by 3 mm, are clearly distinguishable from the two origins of fringe patterns, marked with black crosses.

With the patterns recorded for sample B superimposed with the photograph of the sample (figure 9), the origin of the deformation has been located at a point placed 1.6 mm from the machined step border and 4.35 mm from the upper border of the sample.

After these experiments the superconducting sample properties do not deteriorate. Once the position of the hot

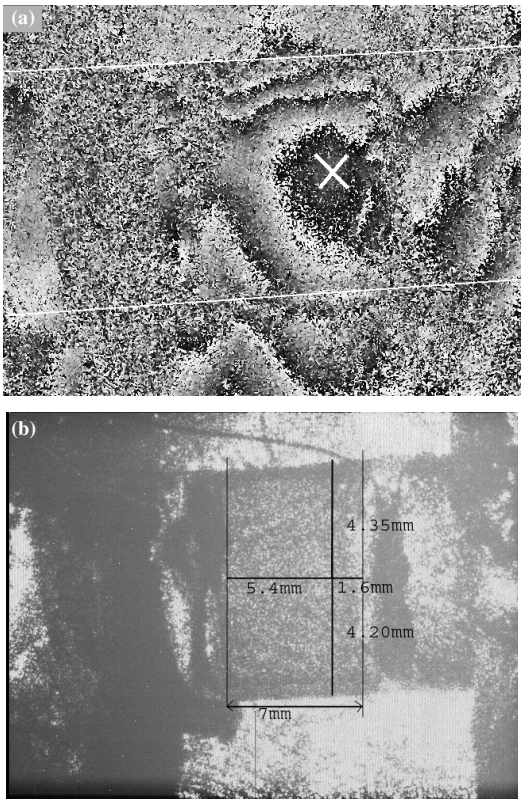

Figure 9. Localization of the position of the hot spot from the point where the fringes have their origin. (a) Origin in the fringe pattern. (b) Position on the sample.

spot is located, microstructural studies have been performed on the sample in order to determine which is the defect in the microstructure that causes this heat generation. The sample has been polished in the longitudinal direction and the

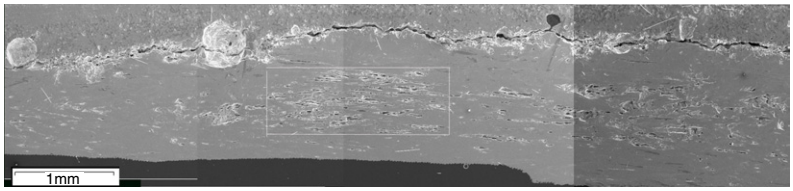

Figure 10. Microstructure of the longitudinal section of sample B at 4.3 mm from the upper border. The agglomerate of holes that are located in the same position where the hot spot has its origin is shown in the photograph.

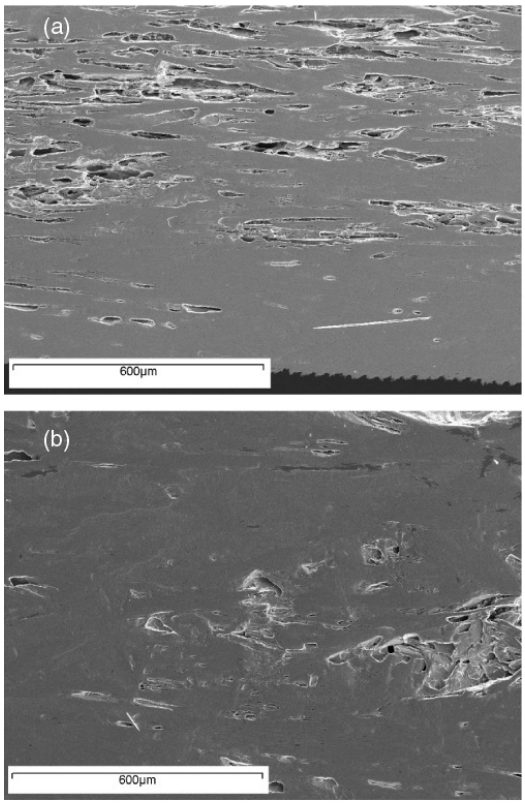

Figure 11. Detail of the microstructure in a region located (a) at 1.5 mm from the border of the machining region and (b) at 3.5 mm. In the first case, the agglomerate of the holes is observed; in the second the microstructure is improved.

microstructure has been analysed with a SEM microscope. The results for a longitudinal section placed at the same distance where the hot spot has been located are presented in figure 10. As is indicated in the micrograph, there is an agglomerate of holes between the superconducting grains that is placed between 1.2 and 2.6 mm from the border of the machined surface and in a depth of 300 μm to 1 mm. A similar structure can be observed 1 mm before the machined step. In this second case, its influence on the sample transport properties is not so important because the maximum in the critical current distribution is located close to the surface and there is enough sample cross-section with good texture between the surface and the holes. However, in the region where the hot spot has its origin, the surface of the sample has been removed and the current is forced to penetrate deeper inside the sample, and, in consequence, the observed defects deteriorate the sample transport properties.

As can be observed in figure 11(a), these holes have their origin in the texturing process. The superconducting grains have a planar geometry and when the misorientation with the texturing direction increases it is more difficult to fill all the volume. The micrograph shows that most of the superconducting paths are destroyed by all the holes that are concentrated in this region. If we move far from this agglomerate of holes (figure 11(b)), the microstructure of the sample improves in the full cross-section, and the superconducting properties of this region should improve in comparison to the region presented in figure 11(a).

6. Conclusions

The heat associated with a hot spot induces a deformation on the sample by dilatation that can be detected using DSPI. This deformation field induces a fringe pattern. With the experimental set-up that has been used in this work, out-of-plane deformations of 0.45 μm/fringe can be detected. This technique has been applied to detect the location of a hot spot before any damage can be caused to the sample.

A further microstructure analysis has revealed that in the samples presented in this study, the hot spot is associated with a region of the sample where many holes are concentrated. The origin of these holes is the texturing process, because in the region where these holes appear, the misorientation of the superconducting grains increases, leading to a more disordered structure.

In consequence, with this technique we can analyse the origin of the hot spots and to modify the processing conditions in order to reduce their effects on the superconducting properties of these materials.

Acknowledgments

This research was supported by the Spanish Ministerio de Educación y Ciencia (MAT2002-04121-C03-01 and -02) and by the Gobierno de Aragón (Applied Superconductivity and Laser Technologies research groups).

References

[1] Verhaege T and Laumond Y 1998 *Fault Current Limiters in Handbook of Applied Superconductivity* vol 2, ed B Seeber (Bristol: Institute of Physics Publishing) pp 1691–702

[2] Giese R F 2003 *Fault Current Limiters in Handbook of Superconducting Materials* vol 2, ed D A Cardwell and D S Ginley (Bristol: Institute of Physics Publishing) pp 1625–32

[3] Leung E M 2000 Superconducting fault current limiters *IEEE Power Eng. Rev.* **20** (Aug.) 15–8, 30
[4] Tixador P *et al* 2000 Quench in bulk HTS materials: application to the fault current limiter *Supercond. Sci. Technol.* **13** 493–7
[5] Ye L and Juengst K P 2004 Modeling and simulation of high temperature resistive superconducting fault current limiters *IEEE Trans. Appl. Supercond.* **14** 839–42
[6] Noe M, Juengst K P, Werfel F N, Elschner S, Bock J, Breuer F and Kreutz R 2003 Testing bulk HTS modules for resistive superconducting fault current limiters *IEEE Trans. Appl. Supercond.* **13** 1976–9
[7] López-Gascón C I 2005 *PhD Thesis* University of Zaragoza
[8] Mora M, Díez J C, López-Gascón C I, Martínez E and de la Fuente G F 2003 Laser textured Bi-2212 in planar geometries *IEEE Trans. Appl. Supercond.* **13** 3188–91
[9] Mora M, López-Gascón C, Angurel L A and de la Fuente G F 2004 The influence of support temperature on Bi-2212 monoliths textured by diode laser zone melting *Supercond. Sci. Technol.* **17** 1329–34
[10] Mora M, Gimeno F, Angurel L A and de la Fuente G F 2004 Laser zone melted $Bi_2Sr_2CaCu_2O_{8+\delta}$ thick films on (100) MgO substrate *Supercond. Sci. Technol.* **17** 1133–8
[11] Herrmann J, Savvides N, Müller K H, Zhao R, McCaughey G, Darmann F and Apperley M 1998 Current distribution and critical state in superconducting silver-sheathed (Bi,Pb)-2223 tapes *Physica* C **305** 114–24
[12] Lee H, Kim H M, Jankowski J and Iwasa Y 2004 Detection of hot spot in HTS coils and test samples with acoustic emission signals *IEEE Trans. Appl. Supercond.* **14** 1298–301
[13] Park K B, Kang J S, Lee B W, Oh I S, Choi H S, Kim H R and Hyun O B 2003 Quench behavior of YBaCuO films for fault current limiters under magnetic filed *IEEE Trans. Appl. Supercond.* **13** 2092–5
[14] Recuero S, Andrés N, Lobera J, Arroyo M P, Angurel L A and Lera F 2005 Application of DSPI to detect inhomogeneous heating on superconducting ceramics *Meas. Sci. Technol.* **16** 1030–6
[15] Rastogi P K (ed) 2001 *Digital Speckle-Pattern Interferometry and Related Techniques* (New York: Wiley)
[16] Recuero S, Andrés N, Arroyo M P, Lera F and Angurel L A 2005 Superconductor ceramics behavior analyses during service by speckle metrology *Proc. SPIE Optical Measurement Systems for Industrial Inspection* vol 5856 (Bellingham, WA: SPIE Optical Engineering Press) pp 775–85